


## PAPER



Cite this: *Sustainable Energy Fuels*,  
2023, 7, 5565

# Selective regression models for the rapid upgrading of raw sugar into 5-HMF bio-fuel additive under a sustainable/reusable system†

Panya Maneechakr,<sup>\*a</sup> Irwan Kurnia,<sup>b</sup> Asep Bayu,<sup>c</sup> Obie Farobie,<sup>d</sup> Chanatip Samart,<sup>e</sup> Suwadee Kongparakul,<sup>e</sup> Guoqing Guan<sup>f</sup> and Surachai Karnjanakom<sup>g</sup> <sup>\*a</sup>

In this research, catalytic upgrading of commercial sucrose (CS) into 5-hydroxymethylfurfuraldehyde (5-HMF) was carried out using a reusable system with a short reaction time. The catalytic behavior for facile production of 5-HMF was systematically described *via* important factors such as catalyst amount, reaction temperature, reaction time and choline chloride (ChCl) amount. The sulfonic-magnetic-copper carbonized carbon (S@Fe-Cu-C) catalyst was prepared *via* pyrolysis + sulfonation processes, and also specifically characterized in detail. The catalytic capabilities of S@Fe-Cu-C and ChCl were systematically studied, and the results indicated dramatic efficiency for the selective production of 5-HMF from CS conversion *via* hydrolysis, isomerization and dehydration. The highest percent yield of 5-HMF product achieved was 86.7% using experimental design. The S@Fe-Cu-C also exhibited the highest turnover rate for the conversion of CS to 5-HMF when compared with various commercial catalysts. Meanwhile, the reusability of the catalyst was investigated for up to 10 cycles with little change in the 5-HMF yield, and S@Fe-Cu-C and ChCl could be recovered in a good way. This research focuses on the catalytic/reusable capabilities for green production of 5-HMF, and could be further expected to have actual applications in renewable industry.

Received 19th June 2023  
Accepted 19th October 2023

DOI: 10.1039/d3se00788j

rsc.li/sustainable-energy

## 1. Introduction

Due to the large-scale diminution of fossil fuels in the environment, the evolution of sustainable techniques for selective production of renewable chemicals/energy is being realized in detail.<sup>1</sup> Herein, biomass resources are regarded as a suitable material for the production of green chemicals due to their worldwide presence in highly abundant amounts.<sup>2</sup> Recently, many kinds of green chemicals, such as formic acid (FA), lactic acid (LA), 5-(hydroxymethyl)furfural (5-HMF), alkyl levulinate

(AL) and others, have been produced using developed synthetic procedures.<sup>3</sup> As a focal point, 5-HMF is an interesting chemical (based on a high value-added chemical), which can be applied for further transformation to 2,5-furandicarboxylic acid (FDCA), 2,5-bis(hydroxymethyl)furan (BHMF), 5-(ethoxymethyl)-2-furfuraldehyde (5-EMF) and/or 2,5-dimethylfuran (DMF).<sup>4,5</sup> As such, sugar is a most suitable substance that can be really converted into the above chemicals, probably due to its uncomplicated structure with reaction requirement.<sup>6–9</sup> Perez *et al.*<sup>10</sup> reported that sugars such as fructose, glucose and sucrose can be easily converted to 5-HMF (with an obtained yield of about 50–90%) and other chemicals using ionic liquids and homogeneous acid catalysts such as [MBCIm]SO<sub>3</sub>Cl, [BMIM]Cl, HCl, HNO<sub>3</sub> and/or H<sub>2</sub>SO<sub>4</sub>. However, there are several issues; for example, it is difficult to be removed out and recovered from the reaction system. Also, it cannot be totally reused due to the similar characteristics of the liquid phase.<sup>11</sup> Meanwhile, the further hydration and polymerization of 5-HMF to form levulinic + formic acids and humins can possibly occur since it strongly requires harsh conditions, such as a large amount of catalyst (>2 times the substrate amount), high temperature (>120 °C) and long reaction time (>60 min). Thus, a sustainable/reusable route for specific production of 5-HMF should be considered in order to overcome the above problems.<sup>12–15</sup>

<sup>a</sup>Department of Chemistry, Faculty of Science, Rangsit University, Pathumthani 12000, Thailand. E-mail: panya.m@rsu.ac.th; surachai.ka@rsu.ac.th

<sup>b</sup>Department of Chemistry, Faculty of Mathematics and Natural Sciences, Universitas Padjadjaran, Jl. Raya Bandung – Sumedang KM. 21 Jatinangor, Sumedang 45363, Indonesia

<sup>c</sup>Research Center for Biotechnology, Indonesian Institute of Sciences (LIPI), Bogor, West Java, Indonesia

<sup>d</sup>Department of Mechanical and Biosystem Engineering, Faculty of Agricultural Engineering and Technology, IPB University (Bogor Agricultural University), IPB Darmaga Campus, Bogor, West Java 16002, Indonesia

<sup>e</sup>Department of Chemistry, Faculty of Science and Technology, Thammasat University, Pathumthani 12120, Thailand

<sup>f</sup>Energy Conversion Engineering Laboratory, Institute of Regional Innovation (IRI), Hirotsuki University, Aomori 030-0813, Japan

† Electronic supplementary information (ESI) available. See DOI: <https://doi.org/10.1039/d3se00788j>

Several researchers are considerably focused on applying and modifying solid acid catalysts, since they can be reused in several cycles when suitable conditions are applied. Recently, Gupta *et al.*<sup>16</sup> found that solid acid-loaded natural zeolite (PMA/NZ) could well catalyze the selective conversion of sugar (glucose and fructose) to 5-HMF at 140 °C for 4 h. Eblagon *et al.*<sup>17</sup> managed to synthesize and apply niobium oxide-phosphorylated carbon xerogel composites for the catalytic production of 5-HMF (30.8% yield) from glucose conversion at 180 °C for 30 min. Wang *et al.*<sup>18</sup> successfully synthesized 5-HMF with a high yield under fructose dehydration at 180 °C for 2 h using a lignin-derived mesoporous carbon. Niakan *et al.*<sup>19</sup> reported that catalytic fructose dehydration to 5-HMF could be well achieved over propylsulfonic acid-modified mesoporous SBA-15. Herein, even these catalysts present good catalytic activity for 5-HMF production with a range of about 30–70% yield, but the separation process is still complicated *via* centrifugation/filtration techniques, leading to long operation time and high operation cost. The utilization of magnetic material (Fe<sub>3</sub>O<sub>4</sub>) can be regarded as an interesting alternative to solve the above mentioned issues, since it has excellent physicochemical stability for catalytic reactions, and can also be easily separated from the reaction system by using an exterior magnetic field.<sup>20</sup> Unfortunately, due to only Lewis acid sites existing on pristine magnetic material, the catalytic production of 5-HMF from sugar conversion may not be totally achieved since Brønsted acid sites on the catalyst are required for some reactions, such as hydrolysis and dehydration. The modification of the active sites on magnetic materials should be considered as a promising alternative route for this research field. Hu *et al.*<sup>20</sup> studied a method for the preparation of a magnetic lignin-derived carbonaceous catalyst, and applied it for the dehydration of fructose into 5-HMF in DMSO with notable catalytic efficiency and reusability. Karimi *et al.*<sup>21</sup> prepared a propyl sulfonic acid-functionalized magnetic graphene oxide nanocomposite *via* a covalent immobilization technique, leading to facile/fast separation by a magnet after complete reactions for 5-HMF production. Le *et al.*<sup>22</sup> discussed that sulfonated magnetic carbon nanoparticles not only give a yield of 5-HMF (51.6%) from fructose conversion at 180 °C for 30 min, but also presented good recyclability of the catalyst up to three cycles. However, some undesired features still occurred, such as high production cost for 5-HMF in the high temperature range of about 120–180 °C. In this case, the 5-HMF yield can be reduced to some extent by further transformation and degradation into undesirable products, such as acidic compounds, humins and/or complex polymers. Also, many research studies focus on using fructose as a starting feedstock for facile production of 5-HMF because it can be obtained with a high yield. But in fact, it still requires industrial operation costs for CS conversion into fructose *via* hydrolysis and isomerization processes first.

To solve the issues mentioned above, in this study, 5-HMF was easily produced from the one-step conversion of CS using a reusable process over sulfonic-magnetic-copper carbonized carbon (S@Fe-Cu-C). Here, a deep eutectic solvent (DES) was also applied for a new generation of recycling process based on remarkable properties such as low vapor pressure/melting

points, high thermal stability, good biodegradability and environmental friendliness.<sup>23</sup> The DES integration in the presence of ChCl + MeCN + S@Fe-Cu-C was newly developed and systematically studied for facile/fast/selective production of 5-HMF from CS conversion. The S@Fe-Cu-C was specifically characterized using BET, XRD, SEM-EDS, VSM, XPS, TGA, NH<sub>3</sub>-TPD and Py-FTIR techniques. The 5-HMF production and its possible mechanism were carefully studied and discussed *via* optimization techniques. The turnover rate of S@Fe-Cu-C for CS conversion was examined with commercial solid acid catalysts such as Alumina, H-ZSM-5, SiO<sub>2</sub>-Tosic acid and Amberlyst-55. Finally, the S@Fe-Cu-C catalyst was tested for reusability and stability for 10 cycles without a restoration procedure.

## 2. Experimental

### 2.1. Synthesis of the catalyst support (Fe-Cu-C)

In brief, a definite amount of dried Ulva powder was added into a solution consisting of iron trichloride and copper dichloride at a molar ratio of 10 Fe to 1 Cu. The mixed solution was then continuously stirred for 2 h, followed by a drying procedure at 100–110 °C. After complete impregnation, the pyrolysis of the dried sample was carried out at 550 °C for 1 h under nitrogen flow.<sup>24</sup> Here, magnetic-copper carbonized carbon (Fe-Cu-C) was obtained.

### 2.2. Synthesis of the active catalyst (S@Fe-Cu-C)

In brief, a definite ratio of synthesized Fe-Cu-C and sulfuric chlorohydrin (SC) was added into ethanol (50 mL) under a reflux set-up.<sup>25</sup> The mixed solution was then continuously stirred for 6 h under nitrogen flow. After complete sulfonation, the S@Fe-Cu-C catalyst was separated, and cleaned with distilled water, followed by a drying procedure in an oven at 105 °C. Herein, the synthesized S@Fe-Cu-C catalysts were named as S0@Fe-Cu-C, S1@Fe-Cu-C, S2@Fe-Cu-C and S3@Fe-Cu-C based on the weight ratios of SC to Fe-Cu-C of 0 : 1, 1 : 1, 2 : 1 and 3 : 1, respectively. In addition, the synthesis procedures of the S@Fe-Cu-C catalysts were summarized in each step (Fig. S1†).

### 2.3. Catalyst characterization

The procedures for the characterization of the S@Fe-Cu-C catalysts using BET, XRD, SEM-EDS, VSM, XPS, TGA, NH<sub>3</sub>-TPD and Py-FTIR techniques are provided in the ESI (ESI)†.

### 2.4. Catalytic experiment

The selective production of 5-HMF from CS conversion catalyzed by S@Fe-Cu-C was proceeded using the traditional reflux technique. In short, the exact amounts of CS and S@Fe-Cu-C were added into a mixture of acetonitrile (MeCN) and ChCl contained in a 100 mL glass tube (closed system). The reaction conditions were systematically determined using experimental design. After finishing the process, before ChCl was recrystallized at a cool temperature, the spent S@Fe-Cu-C catalyst should be rapidly separated out from the system using an outward magnet. Meanwhile, the 5-HMF formed in the MeCN layer was easily separated out after recrystallizing ChCl. Before

the reusability test, the spent ChCl and S@Fe-Cu-C were carefully washed with butanone to remove some adsorbed organic chemicals from their surfaces/structures.<sup>26</sup>

### 2.5. Experimental design for 5-HMF production over the S@Fe-Cu-C catalyst

Several advantages from experimental design were found; for instance, (I) it could decrease some error in determining the influence of each parameter and their interactions, (II) the production cost of 5-HMF could be significantly reduced since a lower number of experiments were carried out by DOE, and (III) much more optimum conditions and response of the yield could be obtained when compared with the conventional experiments.<sup>27</sup> The effects of independent input parameters such as  $X_1$  = ChCl adding amount (g),  $X_2$  = S@Fe-Cu-C adding amount (g),  $X_3$  = reaction temperature (°C) and  $X_4$  = reaction time (min) on the response of 5-HMF yield were investigated to find the significant levels using  $2^k$  factorial design at a 95% confidence level. The ranges of factorial design consisting of sixteen experiments with low (−1) and high (1) levels are shown in Table 1. The regression model for determining the effect of each parameter was provided as follows in eqn (1):

$$Y = \beta_0 + \sum_{i=1}^k \beta_i X_i + \sum_{i < j} \sum \beta_{ij} X_i X_j \quad (1)$$

where  $Y$  is the percentage of 5-HMF yield,  $\beta_0$  is the intercept/constant coefficient,  $\beta_i$  is the linear coefficient,  $\beta_{ij}$  is the interaction coefficient of each parameter and  $X_i$  and  $X_j$  are the codes of independent input parameters.

The optimization of the synthesis of 5-HMF and the responses under a deep eutectic solvent-biphasic system were designed by using three levels of Box–Behnken model based on

quadratic/response surface methodology. This model was defined from a combination of factorial with incomplete block designs, presented in the shape of a box. Meanwhile, the internal structure of the box was assigned by a wire frame, which constituted the edges of the box. The number of experiments in this design was fixed as  $N_{\text{exp}} = 2N_p(N_p - 1) + N_{\text{cp}}$ , where  $N_{\text{exp}}$  is the number of experiments,  $N_p$  is the number of input parameters and  $N_{\text{cp}}$  is the number of central points.<sup>28</sup> The ranges of this design consisting of fifteen experiments with low (−1), medium (0) and high (1) levels are shown in Table 2. The quadratic model for maximizing the 5-HMF yield was provided as follows in eqn (2):

$$Y = \beta_0 + \beta_1 X_1 + \beta_2 X_2 + \beta_3 X_3 + \beta_{11} X_1^2 + \beta_{22} X_2^2 + \beta_{33} X_3^2 + \beta_{12} X_1 X_2 + \beta_{13} X_1 X_3 + \beta_{23} X_2 X_3 \quad (2)$$

where  $Y$  is the percentage of 5-HMF yield,  $\beta_0$  is the intercept/constant coefficient,  $\beta_1$ ,  $\beta_2$  and  $\beta_3$  are the linear coefficients,  $\beta_{11}$ ,  $\beta_{22}$  and  $\beta_{33}$  are the quadratic coefficients,  $\beta_{12}$ ,  $\beta_{13}$  and  $\beta_{23}$  are the interaction coefficients of each parameter and  $X_1$ ,  $X_2$  and  $X_3$  are the codes of independent input parameters.

### 2.6. 5-HMF analysis

The 5-HMF products were determined by an Agilent 1200 high performance liquid chromatography (HPLC) system, operating with an ultraviolet (UV) detector at 284 nm, an analytical column at 30 °C and a mobile phase of water/methanol (0.8/0.2 (v/v)). The CS conversion was determined by an Aminex HPX-87H column, operating with a Refractive Index (RI) detector and analytical column at 65 °C using 0.05 M H<sub>2</sub>SO<sub>4</sub> as a mobile phase at a flow rate of 0.55 mL min<sup>−1</sup>. The amount of 5-HMF product (%mol) were calculated based on an external standard method.<sup>29</sup> To confirm their reproducibility, each experiment was repeated at least 3 times under the same conditions.

**Table 1** Experimental investigation of 5-HMF production derived from  $2^4$  factorial design<sup>a</sup>

Run	$X_1$ (g)	$X_2$ (g)	$X_3$ (°C)	$X_4$ (min)	5-HMF yield (%)
1	1.2 (−1)	0.2 (−1)	80 (−1)	60 (−1)	45.4
2	6.0 (−1)	0.2 (−1)	80 (−1)	60 (−1)	51.5
3	1.2 (−1)	1.4 (1)	80 (−1)	60 (−1)	45.0
4	6.0 (−1)	1.4 (1)	80 (−1)	60 (−1)	61.2
5	1.2 (−1)	0.2 (−1)	130 (1)	60 (−1)	49.4
6	6.0 (−1)	0.2 (−1)	130 (1)	60 (−1)	59.2
7	1.2 (−1)	1.4 (1)	130 (1)	60 (−1)	51.8
8	6.0 (−1)	1.4 (1)	130 (1)	60 (−1)	76.0
9	1.2 (−1)	0.2 (−1)	80 (−1)	120 (1)	46.0
10	6.0 (−1)	0.2 (−1)	80 (−1)	120 (1)	50.9
11	1.2 (−1)	1.4 (1)	80 (−1)	120 (1)	40.8
12	6.0 (−1)	1.4 (1)	80 (−1)	120 (1)	62.0
13	1.2 (−1)	0.2 (−1)	130 (1)	120 (1)	48.9
14	6.0 (−1)	0.2 (−1)	130 (1)	120 (1)	58.8
15	1.2 (−1)	1.4 (1)	130 (1)	120 (1)	52.5
16	6.0 (−1)	1.4 (1)	130 (1)	120 (1)	80.2

<sup>a</sup> The factors are coded as follows:  $X_1$  = ChCl adding amount (g),  $X_2$  = S@Fe-Cu-C adding amount (g),  $X_3$  = reaction temperature (°C) and  $X_4$  = reaction time (min).

**Table 2** Experimental investigation of 5-HMF production derived from Box–Behnken design<sup>a</sup>

Run	$X_1$ (g)	$X_2$ (g)	$X_3$ (°C)	5-HMF yield (%)	
				Observed	Predicted
1	1.2 (−1)	0.2 (−1)	105 (0)	59.0	59.9
2	6.0 (1)	0.2 (−1)	105 (0)	65.2	62.1
3	1.2 (−1)	1.4 (1)	105 (0)	58.9	62.0
4	6.0 (1)	1.4 (1)	105 (0)	70.6	69.7
5	1.2 (−1)	0.8 (0)	80 (−1)	69.2	66.2
6	6.0 (1)	0.8 (0)	80 (−1)	72.3	73.3
7	1.2 (−1)	0.8 (0)	130 (1)	69.3	68.3
8	6.0 (1)	0.8 (0)	130 (1)	68.2	71.2
9	3.6 (0)	0.2 (−1)	80 (−1)	73.7	75.8
10	3.6 (0)	0.2 (−1)	80 (−1)	75.3	75.3
11	3.6 (0)	1.4 (1)	130 (1)	70.4	70.4
12	3.6 (0)	1.4 (1)	130 (1)	82.8	80.7
13	3.6 (0)	0.8 (0)	105 (0)	85.1	85.1
14	3.6 (0)	0.8 (0)	105 (0)	85.4	85.1
15	3.6 (0)	0.8 (0)	105 (0)	84.8	85.1

<sup>a</sup> The factors are coded as follows:  $X_1$  = ChCl addition amount (g),  $X_2$  = S@Fe-Cu-C addition amount (g) and  $X_3$  = reaction temperature (°C).

### 3. Results and discussion

#### 3.1. Catalyst characterization results

The investigation of the  $N_2$  sorption behaviors *via* isotherms and porous distributions of the S@Fe-Cu-C catalysts at different weight ratios of SC to Fe-Cu-C are provided in Fig. 1. As represented in Fig. 1A, all of the prepared catalysts exhibited IUPAC (type IV) isotherms, which were specific to mesoporous materials. It should be noted that a few micropores might have generally existed since high adsorption capacity at low adsorbate pressure was found for all catalysts. Remarkably, the capacity of the hysteresis loop found in each isotherm decreased when the weight ratios of SC to Fe-Cu-C increased, resulting from the substantial existence of sulfonic groups on the porous catalysts.<sup>30</sup> For Fig. 1B, the range of porous distribution in each catalyst had no notable change, indicating that the functionalization process in this study had no effect on porous blockage nature.<sup>31</sup> These BET-BJH results were well supported in detail as shown in Table 3. Here, the surface area and pore volume decreased from 598.1 to 522.7  $m^2 g^{-1}$  and 1.11 to 0.78  $cm^3 g^{-1}$ , respectively, when the weight ratios of SC to Fe-Cu-C were increased in series.

The SEM result of S2@Fe-Cu-C is provided in Fig. 2A. It is clearly observed that S2@Fe-Cu-C presented an irregular morphology. Meanwhile, no bulks/particles of iron and/or copper oxides were clearly found on the S2@Fe-Cu-C surface, indicating that the dispersive natures of these oxides were good during the preparation process.<sup>32</sup> In Fig. 2B–E, the EDX results confirm that the actual existence of sulfur, iron and copper elements was detected with a valid distribution on the S2@Fe-Cu-C structure. Fig. 3 shows the XRD results of the S@Fe-Cu-C catalysts at different weight ratios of SC to Fe-Cu-C. One can

observe that the reflective peaks of the magnetic structure were found at about 30, 35, 44, 54, 57 and 63° while the intensity peaks were notably decreased with an increase in the weight ratio of SC to Fe-Cu-C, suggesting that sulfonic groups were well covered on the S@Fe-Cu-C structure.<sup>33,34</sup> It should be remarked here that no reflective peak of copper oxide was detected, resulting from a small loading amount as well as very small particle sizes.

The FT-IR spectra of S2@Fe-Cu-C are shown in Fig. 4A. As expected, the major FT-IR peaks of the organic compounds in S2@Fe-Cu-C at wavenumbers of about 3400, 1600, 1370, 1100 and 1020  $cm^{-1}$  were detected, belonging to sulfonic, carboxylic and phenolic groups on the catalyst structure.<sup>35</sup> Meanwhile, the FT-IR peaks of magnetic and copper oxides were found at around 550 and 510  $cm^{-1}$ , respectively.<sup>36</sup> The XPS spectrum of S2@Fe-Cu-C is shown in Fig. 4B–E. As detected, (I) the peaks of S 2p were detected at 168.8 (S=O) and 167.6 (C–S) eV; (II) the peaks of O 1s were detected at 533.5 (C=O), 532.8 (S=O), 531.8 (C–O), 531.1 (Cu–O) and 530.4 (Fe–O) eV; (III) the peaks of Fe 2p were detected at 710.8 ( $Fe^{2+}$ ), 712.0 ( $Fe^{3+}$ ), 723.8 ( $Fe^{2+}$ ) and 725.9 ( $Fe^{3+}$ ) eV; (IV) the peaks of Cu 2p were detected at 934.1 ( $Cu^+$ ), 943.0 ( $Cu^{2+}$ ), and 953.9 ( $Cu^0$ ) eV. The FT-IR and XPS results confirm that the active sites in S2@Fe-Cu-C were well present for the catalytic reaction.<sup>37–40</sup>

The  $NH_3$ -TPD results of the S@Fe-Cu-C catalysts at different weight ratios of SC to Fe-Cu-C are presented in Fig. 5A. Here, only two TPD peaks were basically classified as two kinds of acid sites. A lower temperature range of about 75–200 °C for ammonia desorption was observed for weak acidic sites, while that for strong acidic sites was at a higher temperature of 200–300 °C. For S0@Fe-Cu-C, one main peak at low temperature was detected, belonging Lewis acidic sites. It should be

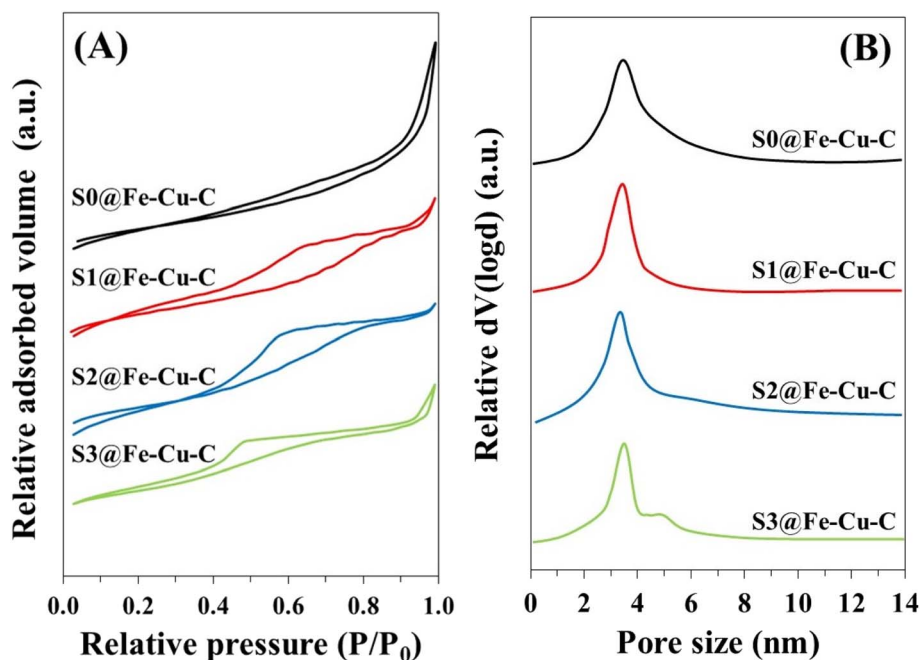


Fig. 1 (A)  $N_2$  sorption isotherms and (B) pore size distributions of the S@Fe-Cu-C catalysts at different weight ratios of SC to Fe-Cu-C.



Table 3 Physical and chemical properties of various as-prepared catalysts

Catalyst	Surface area (m <sup>2</sup> g <sup>-1</sup> )	Pore volume (cm <sup>3</sup> g <sup>-1</sup> )	Pore size (nm)	Acidity (mmol g <sup>-1</sup> )
S0@Fe-Cu-C	598.1	1.11	3.45	1.86
S1@Fe-Cu-C	583.4	1.03	3.44	2.97
S2@Fe-Cu-C	565.3	0.92	3.41	3.58
S3@Fe-Cu-C	522.7	0.78	3.42	3.21
Spent S2@Fe-Cu-C <sup>a</sup>	548.1	0.67	3.12	3.50

<sup>a</sup> After reusability test for 10 cycles.

remarked here that Lewis acidic sites were generally generated by compositions of magnetic and copper oxides present in the catalyst structure. Remarkably, after increasing the weight ratios of SC to Fe-Cu-C from 0:1 to 2:1, the ammonia desorption peak at high temperature was continuously

increased, suggesting that Brønsted acid sites were greatly introduced on the catalyst structure *via* a functionalization procedure of sulfonic acid groups. Unexpectedly, the pattern of ammonia TPD peak was notably changed for S3@Fe-Cu-C when compared with S1@Fe-Cu-C and S2@Fe-Cu-C. This might have

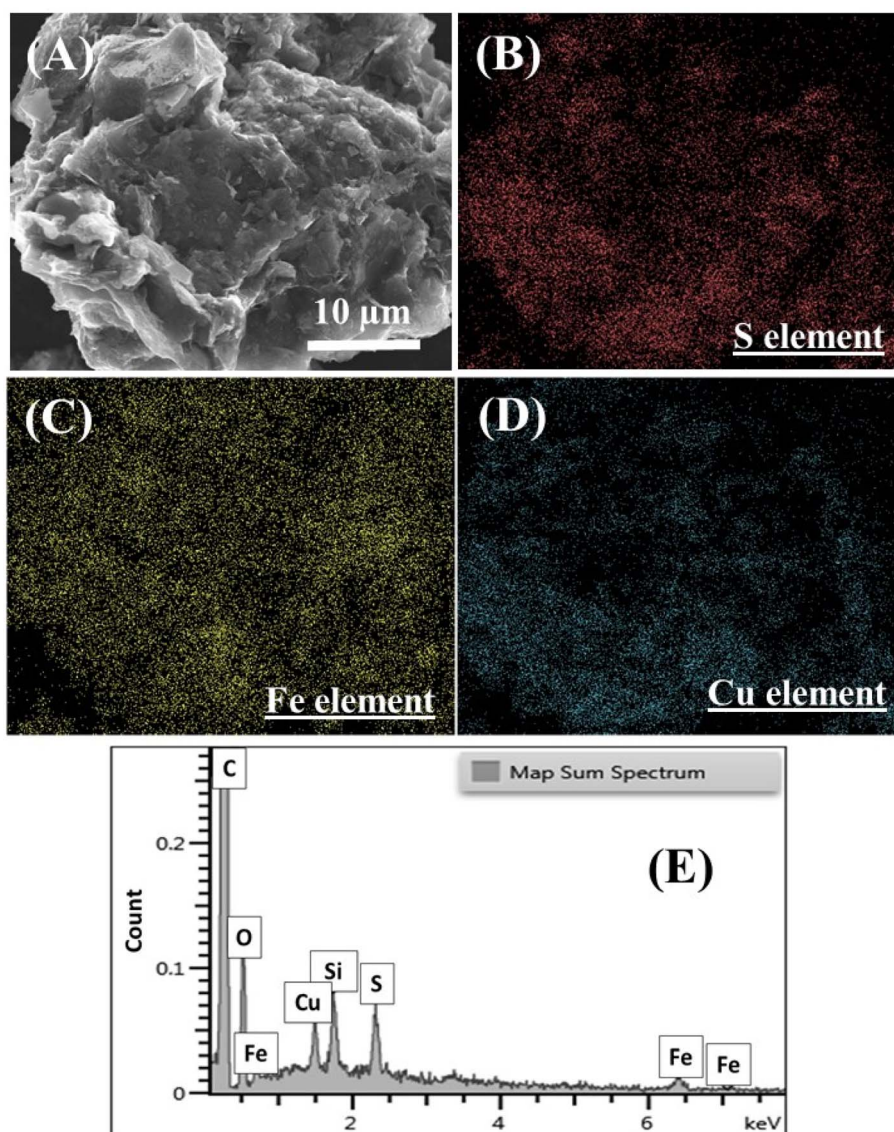


Fig. 2 (A) SEM image, (B–D) EDS mapping images and (E) EDS spectrum of S2@Fe-Cu-C.

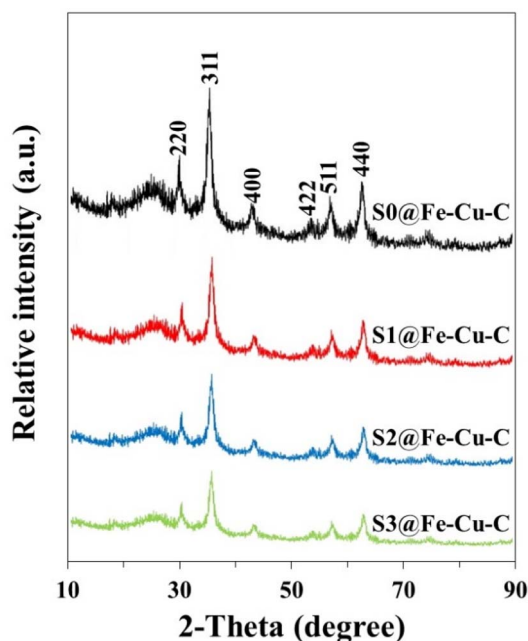


Fig. 3 XRD patterns of the S@Fe-Cu-C catalysts at different weight ratios of SC to Fe-Cu-C.

resulted from over loading of sulfonic acid groups on the catalyst, leading to significant destruction of the catalyst structure during the preparation procedure. Based on these  $\text{NH}_3$ -TPD results, their acidities were well supported in detail as

shown in Table 3. Here, the total acidities were increased from 1.86 to 3.58  $\text{mmol g}^{-1}$  with an increase in their weight ratios of SC to Fe-Cu-C from 0 : 1 to 2 : 1, while the acidity of S3@Fe-Cu-C was 3.21  $\text{mmol g}^{-1}$ . The Py-FTIR spectra results of the S@Fe-Cu-C catalysts at different weight ratios of SC to Fe-Cu-C are presented in Fig. 5B. It should be remarked here that three major peaks at vibrating wavenumbers of about 1450, 1490 and 1545  $\text{cm}^{-1}$  were specifically correlated to Lewis acidic, Lewis-Brønsted acidic and Brønsted acidic positions, respectively.<sup>35,41</sup> As anticipated, more loading amount of sulfonic groups on the catalyst, such as S1@Fe-Cu-C and S2@Fe-Cu-C, could greatly enhance in number/position the Brønsted acidity with their intensity peaks. The obtained results from Py-FTIR were in good agreement with the  $\text{NH}_3$ -TPD survey. The additional results and discussion of TGA and VSM are provided in SI (Fig. S2 and S3<sup>†</sup>). Based on these characterization results, the existence of active sites on the S@Fe-Cu-C catalyst, including Brønsted and Lewis acid sites, was highly useful for catalytic reactions, especially for hydrolysis, isomerization and dehydration reactions.

### 3.2. Catalytic design for 5-HMF production

Since S2@Fe-Cu-C had the highest acidity, it was applied for all catalytic reactions. Table 1 shows the results of 5-HMF production from CS conversion over S@Fe-Cu-C in each batch experiment *via* 2<sup>4</sup> factorial design using a rectilinear model. As shown by the results, the product yields of 5-HMF produced from CS conversion over the S@Fe-Cu-C catalyst were in the range of about 40–80%. As represented in Fig. 6, the probability plots were investigated to primarily scrutinize the significant

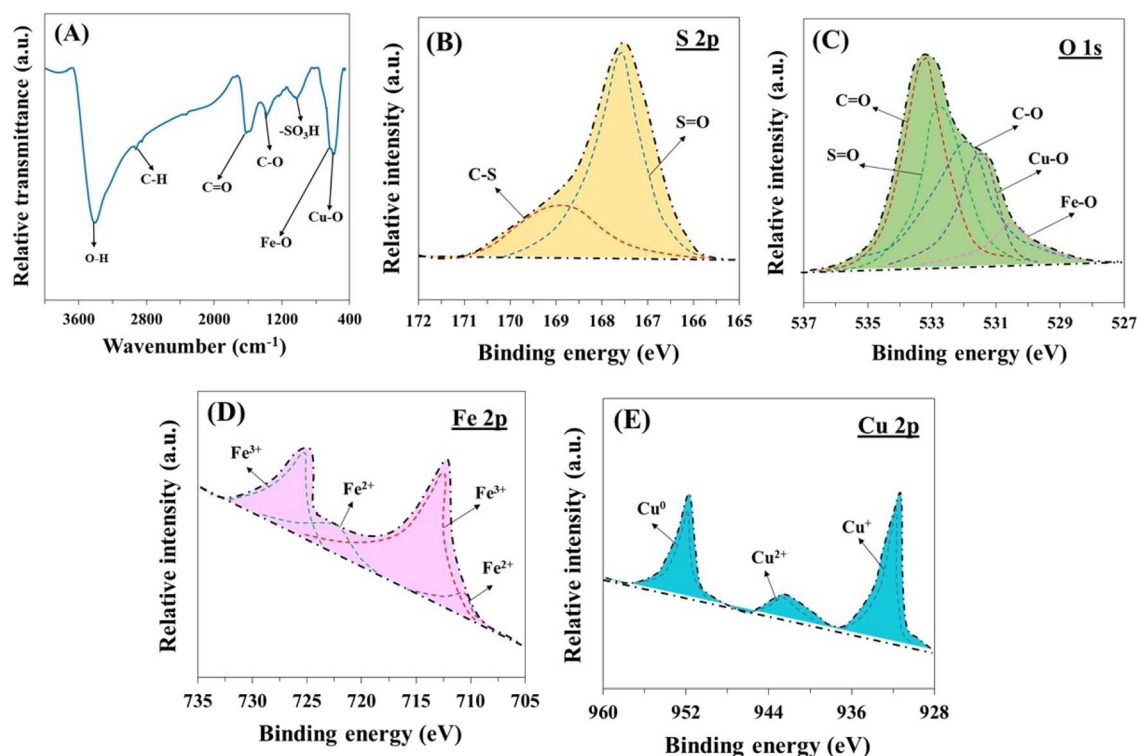


Fig. 4 (A) FT-IR spectra of S2@Fe-Cu-C. XPS spectra of S2@Fe-Cu-C: (B) S 2p, (C) O 1s, (D) Fe 2p and (E) Cu 2p.

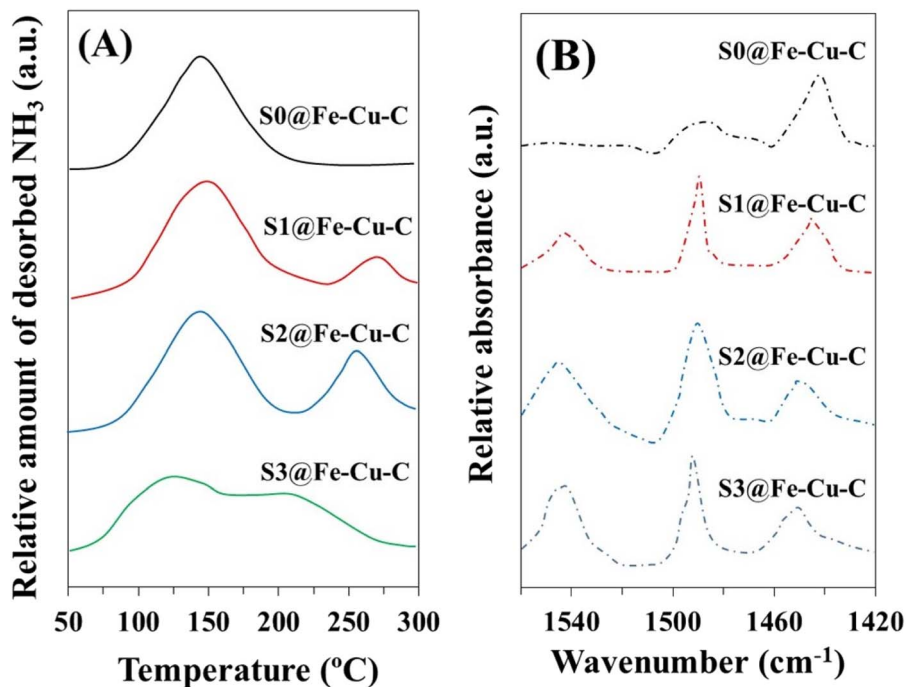


Fig. 5 (A)  $\text{NH}_3$ -TPD profiles and (B) pyridine-FTIR spectra of the  $\text{S@Fe-Cu-C}$  catalysts at different weight ratios of SC to Fe-Cu-C.

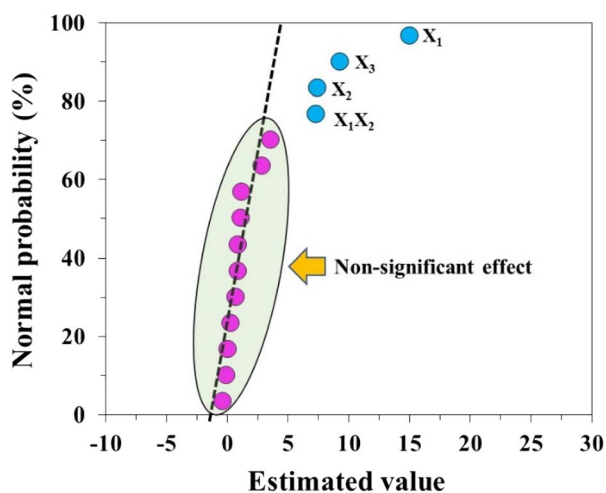


Fig. 6 Normal probability plot for the catalytic production of 5-HMF from CS conversion over  $\text{S@Fe-Cu-C}$ .

factors for 5-HMF production. One can survey that three significant factors, namely ChCl addition amount ( $X_1$ ),  $\text{S@Fe-Cu-C}$  addition amount ( $X_2$ ) and reaction temperature ( $X_3$ ), including  $X_1X_2$  interaction between the added amount of ChCl and  $\text{S@Fe-Cu-C}$ , had a great impact on the yield of 5-HMF. The major sequence of each factor that affected catalytic production of 5-HMF from CS conversion was ChCl addition amount > reaction temperature >  $\text{S@Fe-Cu-C}$  addition amount. It should be remarked here that the range of reaction time (60 to 120 min) had no notable effect for increasing the yield of 5-HMF. Actually, a long reaction time was highly needed for 5-HMF formation by our conventional system, but it could lead to further

production of polymeric humins *via* general condensation or polymerization.<sup>42</sup> This indicated that fast production of 5-HMF was well achieved in this work *via* the excellent catalytic system. Thus, the catalytic production of 5-HMF in the shortest reaction time of 1 h was conditionally fixed for all catalytic testing. Table 4 shows the variance analysis for the catalytic production of 5-HMF from CS conversion over  $\text{S@Fe-Cu-C}$  under a precise level at 95% ( $F_{0.05}$ ).

In addition, the maximal and minimal  $F$ -values were 900.30 and 220.67, belonging to ChCl addition amount and  $\text{S@Fe-Cu-C}$  addition amount, respectively. It should be remarked here that ChCl and  $\text{S@Fe-Cu-C}$  should be loaded with suitable amounts. These analysis results were in good agreement with the survey of normal probability as shown in Fig. 6. From these results, the predicted 5-HMF yield was carefully calculated *via* a rectilinear model, and provided as follows in eqn (3):

$$Y = 54.99 + 7.501X_1 + 3.714X_2 + 4.626X_3 + 3.661X_1X_2 \quad (3)$$

where  $Y$  is the 5-HMF yield (%),  $X_1$  is the ChCl addition amount (g),  $X_2$  is the  $\text{S@Fe-Cu-C}$  addition amount (g) and  $X_3$  is the reaction temperature ( $^{\circ}\text{C}$ ).

The probability and distribution plots of the residuals are provided in Fig. 7. As found, the rectilinear model had great preciseness with  $R^2 > 0.9$  (variance level = 98.39%), while the distribution behavior was devoid of anomaly characteristic. From this factorial design, the shortest reaction time (60 min) was chosen for the next step on optimization of 5-HMF production from CS conversion over  $\text{S@Fe-Cu-C}$  *via* Box-Behnken design with a quadratic model. Table 2 represents the experimental results of optimum production of 5-HMF from CS conversion over  $\text{S@Fe-Cu-C}$ . The predicted 5-HMF yield was

**Table 4** Analysis of variance (ANOVA) determined from  $2^4$  factorial design for the catalytic production of 5-HMF from CS conversion over S@Fe-Cu-C<sup>a</sup>

Source of variation	Sum of square	Degree of freedom	Mean square	$F_{\text{value}}$	$F_{\text{critical}}$
$X_1$	900.30	1	900.30	75.76	5.32
$X_2$	220.67	1	220.67	18.57	
$X_3$	342.44	1	342.44	28.82	
$X_4$	0.02	1	0.02	0.00	
$X_1X_2$	214.48	1	214.48	18.05	
$X_2X_3$	52.49	1	52.49	4.42	
Error	106.95	9	11.88	—	
Total	1784.85	15	—	—	

<sup>a</sup> The factors are coded as follows:  $X_1$  = ChCl addition amount (g),  $X_2$  = S@Fe-Cu-C addition amount (mmol),  $X_3$  = reaction temperature ( $^{\circ}\text{C}$ ) and  $X_4$  = reaction time (min).

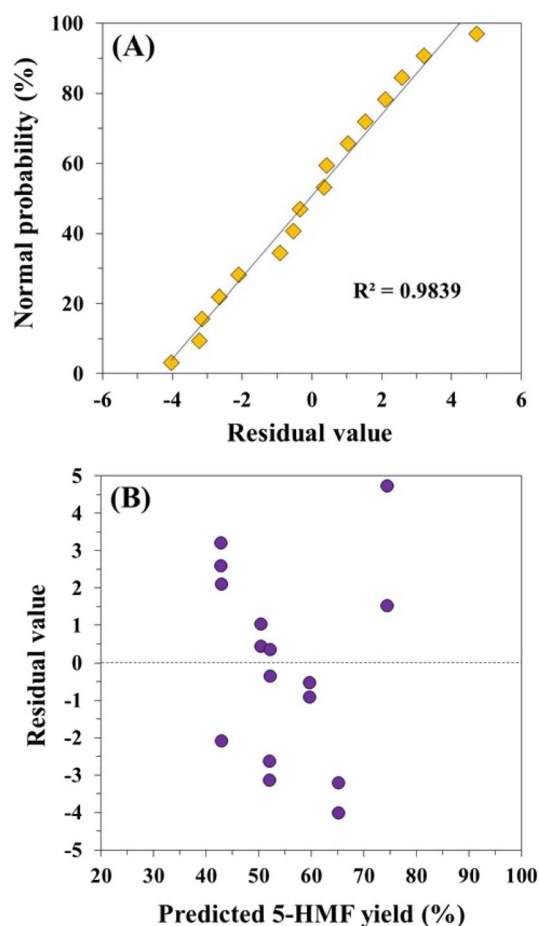


**Fig. 7** (A) Normal probability plot of residual value and (B) distribution plot of residual versus predicted 5-HMF yield determined from  $2^4$  factorial design for the catalytic production of 5-HMF from CS conversion over S@Fe-Cu-C.

carefully calculated *via* the quadratic regression model, and provided as follows in eqn (4):

$$Y = 85.1 + 2.483X_1 + 2.421X_2 + 0.011X_3 - 13.746X_1^2 - 7.934X_2^2 - 1.614X_3^2 + 1.38X_1X_2 - 1.055X_1X_3 + 2.703X_2X_3 \quad (4)$$

where  $Y$  is the 5-HMF yield (%),  $X_1$  is the ChCl addition amount (g),  $X_2$  is the S@Fe-Cu-C addition amount (g) and  $X_3$  is the reaction temperature ( $^{\circ}\text{C}$ ).

The predicted yield of 5-HMF was calculated from eqn (4) and the result is shown in Table 2. As shown in Fig. 8, as found, the quadratic model had great preciseness with  $R^2 > 0.9$  (variance level = 95.36%), while the distribution behavior was

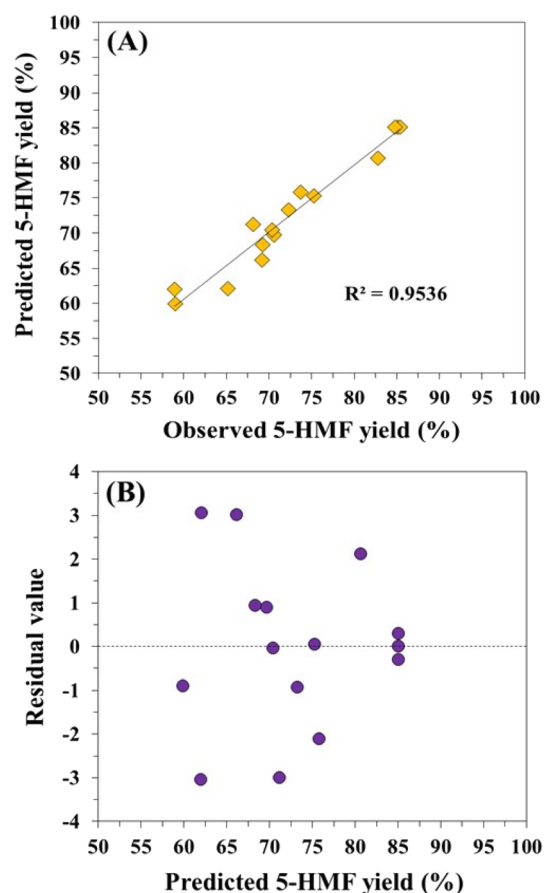


**Fig. 8** (A) Plot of observed versus predicted values of 5-HMF yield and (B) distribution plot of residual value versus predicted 5-HMF yield determined from Box-Behnken design for catalytic production of 5-HMF from CS conversion over S@Fe-Cu-C.



devoid of anomaly characteristics for 5-HMF production in this work. To understand the interaction in each significant factor, the optimization *via* response surface methodology is provided in Fig. 9. The 3D interaction between the ChCl addition amount and S@Fe-Cu-C addition amount for the catalytic production of 5-HMF from CS conversion at a constant value of reaction temperature of 105 °C (medium level) is represented in Fig. 9A. The incremental increase of the ChCl addition amount from 1.2 to 3.6 g could have exclusively enhanced the formation rate of 5-HMF from 68.8 to 85.8%. However, when a ChCl addition amount of >3.6 g and/or a S@Fe-Cu-C addition amount of >0.92 g were used, the 5-HMF yield was obviously decreased, resulting from high viscosity in the mixture system. Also, too many active sites might promote catalytic polymerization of 5-HMF into humins, leading to low selective production of 5-HMF.<sup>43</sup> Interestingly, the existence of ChCl with a suitable amount could suppress the side reactions as well as avoiding its further degradation during the reaction process. Anyway, if too large an amount of ChCl was used, the 5-HMF molecule that might be possibly adsorbed on ChCl recrystallized after finishing the reaction process, resulting in the reduction of the 5-HMF yield. It should be noted that the ChCl crystal was not destroyed even when a large amount of S@Fe-Cu-C (heterogeneous acid catalyst) was added. This was totally different when compared with using HCl (homogeneous acid catalyst).<sup>26</sup> The ChCl molecule

could be easily destroyed when too large an amount of HCl was used, leading to improbability for recrystallization and recycling processes of the spent ChCl. Here, the possible reaction pathways for catalytic conversion of CS into 5-HMF and other products, including their discussion, are thoroughly provided in the SI (Fig. S4†).

In Fig. 9B, the 5-HMF production was maximized at 85.4% from interaction between a ChCl addition amount of 3.6 g with a reaction temperature of 105 °C at a constant value of S@Fe-Cu-C addition amount = 0.8 g (medium level). In the case of Fig. 9C, a little higher yield of 5-HMF (85.6%) was evidently obtained at 105 °C using S@Fe-Cu-C and ChCl amounts of 0.9 and 3.6 g, respectively. It should be remarked here that the reaction temperature used in this study never exceeded 105 °C even though a higher reaction temperature was usually required as a gainful influence, probably due to further conversion of 5-HMF into humins. In addition, active solvent might be evaporated during the reaction when an unsuitable temperature was applied. Thus, experimental design was beneficial for optimal production of 5-HMF from CS conversion over the DES (ChCl + MeCN + S@Fe-Cu-C) system. From these designs, the 5-HMF product could be optimally formed with 86.2% predicted yield under the best conditions, such as ChCl addition amount of 3.82 g, S@Fe-Cu-C addition amount of 0.91 g, reaction temperature of 105 °C and reaction time of 60 min. To confirm

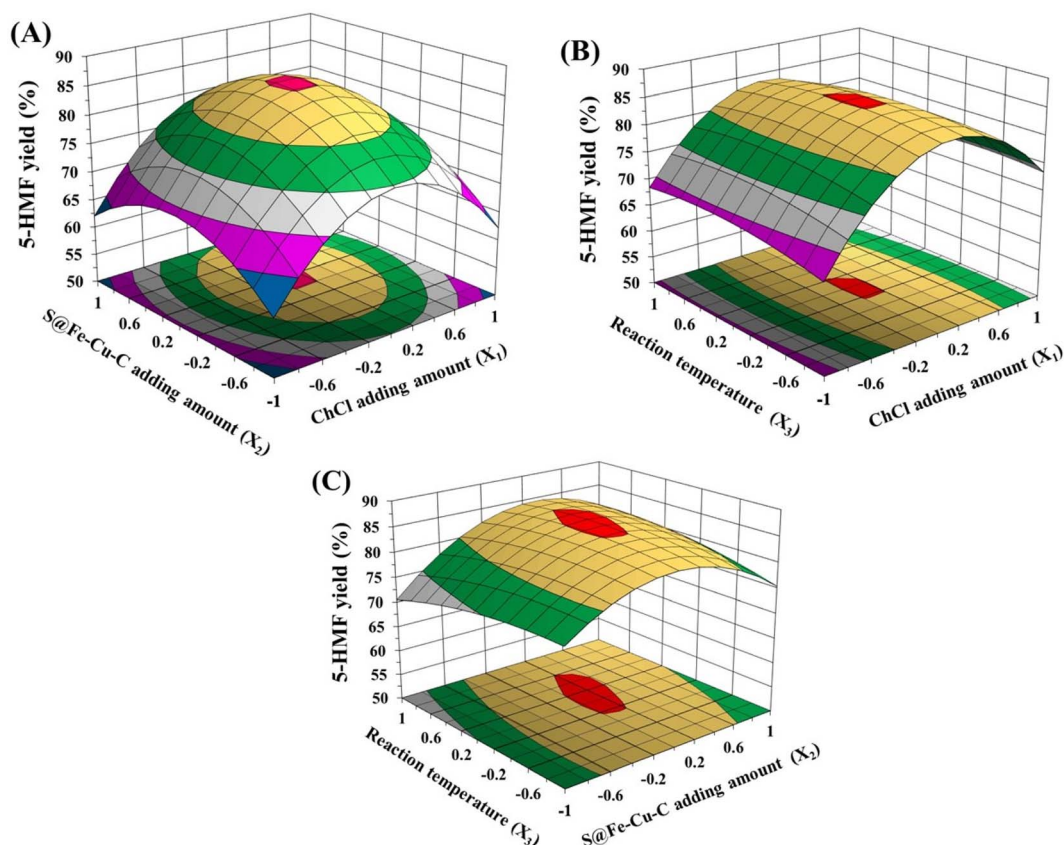


Fig. 9 Response surfaces determined from 5-HMF yield: (A) interaction effect of ChCl and S@Fe-Cu-C addition amount, (B) interaction effect of ChCl addition amount and reaction temperature, and (C) interaction effect of S@Fe-Cu-C addition amount and reaction temperature.

the experimental infallibility, three experiments under the above conditions were performed, and the results evidently found that the actual yield obtained was 86.7%, demonstrating that these designs were reasonable for 5-HMF production. To compare and update, as shown in Table S1 and Fig. S5,<sup>†</sup> the results indicate that our catalytic activity for 5-HMF in current was in a good way.<sup>44–48</sup>

### 3.3. Catalytic reusability

Fig. 10A presents the reusability and stability of S@Fe-Cu-C and ChCl for catalytic conversion of CS into 5-HMF under the optimum conditions obtained in Section 3.2. It is found that a few reductions of 5-HMF yield were detected during the reaction for 10 cycles, demonstrating that the co-application of

S@Fe-Cu-C and ChCl was good for sustainable production of 5-HMF. In contrast, as presented in Fig. 10B, the long-term reusability of H<sub>2</sub>SO<sub>4</sub> with ChCl for selective production of 5-HMF was remarkably lower when compared with using both S@Fe-Cu-C and ChCl. Here, when S@Fe-Cu-C was applied, the percent yield was reduced only 7.3% for 10 cycles while H<sub>2</sub>SO<sub>4</sub> caused a 46.8% reduction in 5-HMF yield. This phenomenon should be attributed to the destruction of the ChCl structure, resulting in low availability of active sites, especially using a homogeneous H<sub>2</sub>SO<sub>4</sub> catalyst. In the case of spent S@Fe-Cu-C, slight deactivation should be due to the adsorption of polymeric intermediates on the active surface.<sup>49</sup> This could be obviously verified from the slight reduction of surface area (from 565.3 to 548.1 m<sup>2</sup> g<sup>-1</sup>) and pore size (from 3.41 to 3.12 nm) of the spent

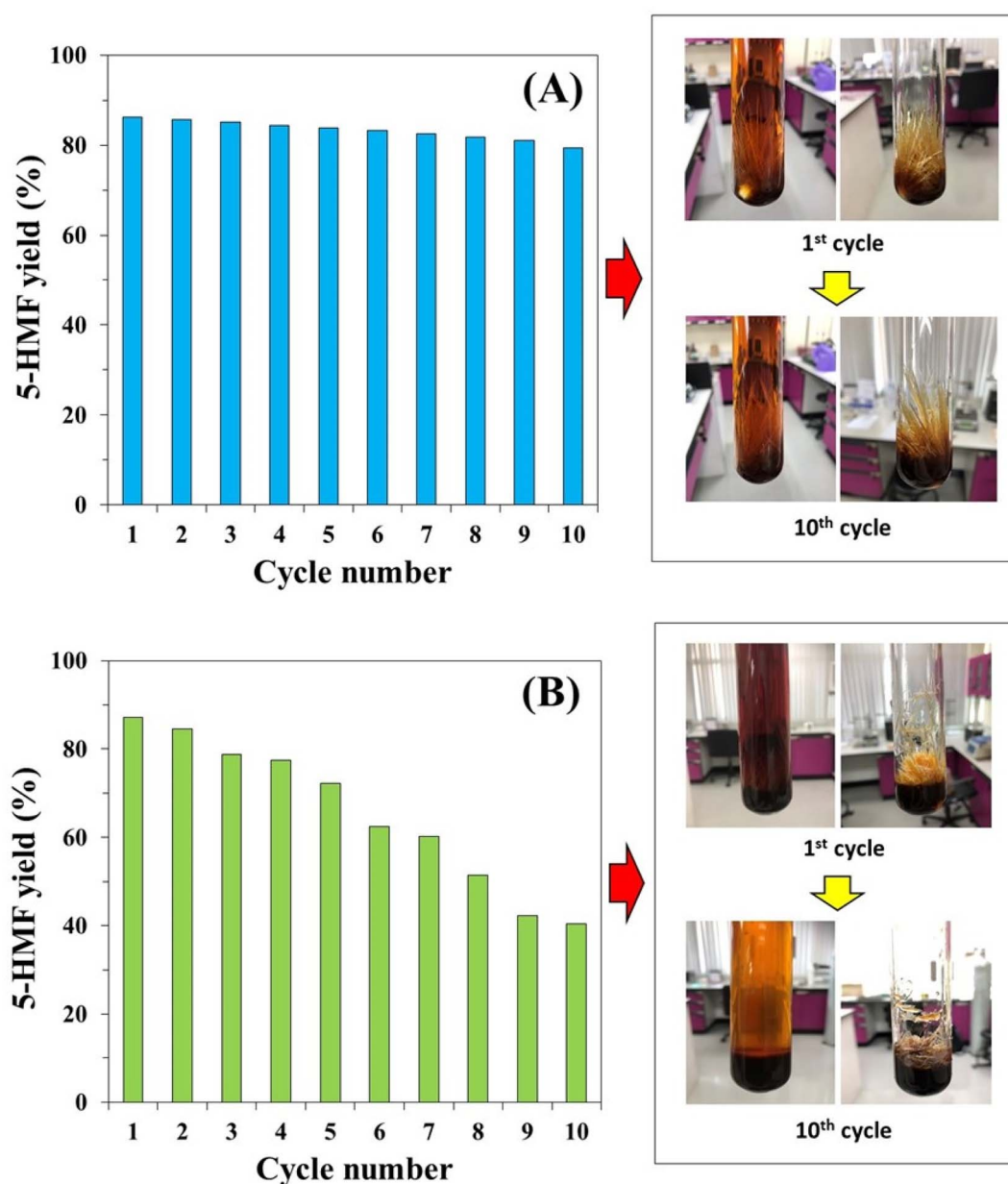


Fig. 10 Catalytic reusability for 5-HMF production from CS conversion using (A) S@Fe-Cu-C and (B) H<sub>2</sub>SO<sub>4</sub>.

catalyst (Table 3). It should be noted here that the acidities of the fresh and spent catalyst were not remarkably different, indicating that no sulfonic leaching significantly occurred during this test.

Here, the amount of H<sub>2</sub>SO<sub>4</sub> added in the reaction system was defined using the same concentration with S@Fe-Cu-C acidity. From the results, one can see that the catalytic performance (ChCl + H<sub>2</sub>SO<sub>4</sub>) based on 5-HMF yield was drastically decreased to some extent with the escalation in recycling number. These phenomena should be attributed to the integrating influence between H<sub>2</sub>SO<sub>4</sub> and ChCl, leading to further transformation of 5-HMF into side products.<sup>50</sup> Remarkably, the efficiencies for ChCl recrystallization and the recycling processes were clearly suppressed when a homogeneous catalyst such as H<sub>2</sub>SO<sub>4</sub> was applied with the escalation of each recycling number. In contrast, the utilization of a heterogeneous catalyst such as S@Fe-Cu-C could well maintain the ChCl recrystallization/recycling processes, including sustainable production of 5-HMF up to ten cycles. Thus, it can be summarized that the as-developed sustainable system was likely preserved for long-term stability/reusability, and had high possibility to be further applied in practical processes for 5-HMF production from CS conversion.

## 4. Conclusions

The preparation of the S@Fe-Cu-C catalyst was achieved, which could be co-applied with ChCl for green production of 5-HMF. The physical and chemical characteristics were summarized in detail. Three factors, namely ChCl addition amount, S@Fe-Cu-C addition amount and reaction temperature, had a great impact on the yield of 5-HMF in this study. Co-application between S@Fe-Cu-C and ChCl was found to be of great usefulness for facile production of 5-HMF in traditional systems. The contribution of magnetic and copper oxide on the catalyst structure perfectly supported catalytic conversion of CS, especially for the isomerization cycle. The 5-HMF product could be actually produced with an average yield of 86.7% under the best conditions, namely ChCl addition amount of 3.82 g, S@Fe-Cu-C addition amount of 0.91 g, reaction temperature of 105 °C and reaction time of 60 min. The reusability test confirmed that the contribution of the heterogeneous catalyst could maintain the perfect stability of the ChCl structure, leading to sustainable production of 5-HMF. This research provided a suitable route for selective production of 5-HMF using green catalysts.

## Conflicts of interest

There are no conflicts to declare.

## Acknowledgements

This research was financially supported by Research Institute of Rangsit University (grant no. 8/2564). The authors wish to acknowledge Department of Chemistry, Faculty of Science, Rangsit University for supporting all instruments and chemicals.

## References

- 1 P. Cao, Y. Li, Y. Li, X. Zhang, X. Wang and Z. Jiang, Surfactant decorated hydrotalcite-supported polyoxometalates for aerobic oxidation of 5-hydroxymethylfurfural and monosaccharides, *Sustainable Energy Fuels*, 2020, **4**, 2236–2248.
- 2 R. Juhola, A. Heponiemi, S. Tuomikoski, T. Hu, H. Prokkola, H. Romar and U. Lassi, Biomass-based composite catalysts for catalytic wet peroxide oxidation of bisphenol A: Preparation and characterization studies, *J. Environ. Chem. Eng.*, 2019, **7**, 1031272.
- 3 A. Das and K. Mohanty, Microwave induced one-pot conversion of d-glucose to 5-hydroxymethylfurfural by a novel sulfate-functionalized Sn-red mud catalyst, *Sustainable Energy Fuels*, 2020, **4**, 6030–6044.
- 4 J. Tacacima, S. Derenzo and J. G. R. Poco, Synthesis of HMF from fructose using Purolite® strong acid catalyst: Comparison between BTR and PBR reactor type for kinetics data acquisition, *Mol. Catal.*, 2018, **458**, 180–188.
- 5 T. Zhang, W. Li, H. Xin, L. Jin and Q. Liu, Production of HMF from glucose using an Al<sup>3+</sup>-promoted acidic phenol-formaldehyde resin catalyst, *Catal. Commun.*, 2019, **124**, 56–61.
- 6 M. Niakan, M. Masteri-Farahani, S. Karimi and H. Shekaari, Sulfonic acid functionalized dendrimer-grafted cellulose as a solid acid catalyst for the high-yield and green production of 5-hydroxymethylfurfural, *Sustainable Energy Fuels*, 2022, **6**, 2514–2522.
- 7 S. Zhou, F. Dai, Y. Chen, C. Dang, C. Zhang, D. Liu and H. Qi, Sustainable hydrothermal self-assembly of hafniumlignosulfonate nanohybrids for highly efficient reductive upgrading of 5-hydroxymethylfurfural, *Green Chem.*, 2019, **21**, 1421–1431.
- 8 Y. Dou, S. Zhou, C. Oldani, W. Fang and Q. Cao, 5-Hydroxymethylfurfural production from dehydration of fructose catalyzed by Aquivion@silica solid acid, *Fuel*, 2018, **214**, 45–54.
- 9 F. Huang, W. Li, Q. Liu, T. Zhang, S. An, D. Li and X. Zhu, Sulfonated tobacco stem carbon as efficient catalyst for dehydration of C6 carbohydrate to 5-hydroxymethylfurfural in  $\gamma$ -valerolactone/water, *Fuel Process. Technol.*, 2018, **181**, 294–303.
- 10 G. P. Perez, A. Mukherjee and M. J. Dumont, Insights into HMF catalysis, *J. Ind. Eng. Chem.*, 2019, **70**, 1–34.
- 11 J. N. Chheda, Y. Román-Leshkov and J. A. Dumesic, Production of 5-hydroxymethylfurfural and furfural by dehydration of biomass-derived mono- and polysaccharides, *Green Chem.*, 2007, **9**, 342–350.
- 12 S. K. Das, S. Chatterjee, S. Mondal and A. Bhaumik, A new triazine-thiophene based porous organic polymer as efficient catalyst for the synthesis of chromenes via multicomponent coupling and catalyst support for facile synthesis of HMF from carbohydrates, *Mol. Catal.*, 2019, **475**, 110483.

- 13 K. Peng, X. Li, X. Liu and Y. Wang, Hydrothermally stable Nb-SBA-15 catalysts applied in carbohydrate conversion to 5-hydroxymethyl furfural, *Mol. Catal.*, 2017, **441**, 72–80.
- 14 L. Wang, H. Guo, Q. Wang, B. Huo, L. Jia, J. Cui and D. Li, The study of active sites for producing furfural and soluble oligomers in fructose conversion over HZSM-5 zeolites, *Mol. Catal.*, 2019, **474**, 110411.
- 15 S. Marullo, C. Rizzo, A. Meli and F. D. Anna, Ionic Liquid Binary Mixtures, Zeolites, and Ultrasound Irradiation: A Combination to Promote Carbohydrate Conversion into 5-Hydroxymethylfurfural, *ACS Sustainable Chem. Eng.*, 2019, **7**, 5818–5826.
- 16 S. Gupta, A. B. Gambhire and R. Jain, Conversion of carbohydrates (glucose and fructose) into 5-HMF over solid acid loaded natural zeolite (PMA/NZ) catalyst, *Mater. Lett.: X*, 2022, **13**, 100119.
- 17 K. M. Eblagon, A. Malaika, K. Ptaszynska, M. F. R. Pereira, M. Kozłowski and J. Figueiredo, Niobium oxide-phosphorylated carbon xerogel composites as solid acid catalysts for cascade conversion of glucose to 5-hydroxymethylfurfural (HMF) in pure water, *Catal. Today*, 2023, **418**, 114070.
- 18 S. Wang, T. L. Eberhardt and H. Pan, Efficient dehydration of fructose into 5-HMF using a weakly-acidic catalyst prepared from a lignin-derived mesoporous carbon, *Fuel*, 2022, **316**, 123255.
- 19 M. Niakan, M. Masteri-Farahani and F. Seidi, Catalytic fructose dehydration to 5-hydroxymethylfurfural on the surface of sulfonic acid modified ordered mesoporous SBA-16, *Fuel*, 2023, **337**, 127242.
- 20 L. Hu, X. Tang, Z. Wu, L. Lin, J. Xu, N. Xu and B. Dai, Magnetic lignin-derived carbonaceous catalyst for the dehydration of fructose into 5-hydroxymethylfurfural in dimethylsulfoxide, *Chem. Eng. J.*, 2015, **263**, 299–308.
- 21 S. Karimi, F. Seidi, M. Niakan, H. Shekaari and M. Masteri-Farahani, Catalytic dehydration of fructose into 5-hydroxymethylfurfural by propyl sulfonic acid functionalized magnetic graphene oxide nanocomposite, *Renewable Energy*, 2021, **180**, 132–139.
- 22 G. T. T. Le, K. Arunaditya, J. Panichpol, T. Rodruangnon, S. Thongratkaew, K. Chaipojjana and K. Faungnawakij, Sulfonated magnetic carbon nanoparticles from eucalyptus oil as a green and sustainable catalyst for converting fructose to 5-HMF, *Catal. Commun.*, 2021, **149**, 106229.
- 23 J. Mehta, A. V. Metre, M. S. Bhakhar, D. S. Panwar and S. Dharaskar, Biomass-derived 5-hydroxymethylfurfural (HMF) and 2,5-dimethylfuran (DMF) synthesis as promising alternative fuel: A prospective review, *Mater. Today: Proc.*, 2022, **62**, 6978–6984.
- 24 W. J. Liu, K. Tian, H. Jiang and H. Q. Yu, Facile synthesis of highly efficient and recyclable magnetic solid acid from biomass waste, *Sci. Rep.*, 2013, **3**, 2419.
- 25 V. Nejadshafiee and M. R. Islami, Adsorption capacity of heavy metal ions using sulfone-modified magnetic activated carbon as a bio-adsorbent, *Mater. Sci. Eng., C*, 2019, **101**, 42–52.
- 26 P. Maneechakr and S. Karnjanakom, Catalytic conversion of fructose into 5-HMF under eco-friendly-biphasic process, *React. Chem. Eng.*, 2020, **5**, 2058–2063.
- 27 S. Karnjanakom and P. Maneechakr, Designs of linear-quadratic regression models for facile conversion of carbohydrate into high value (5-(ethoxymethyl)furan-2-carboxaldehyde) fuel chemical, *Energy Convers. Manage.*, 2019, **196**, 410–417.
- 28 S. Karnjanakom, S. Kongparakul, C. Chaiya, P. Reubroycharoen, G. Guan and C. Samart, Biodiesel production from Hevea brasiliensis oil using SO<sub>3</sub>H-MCM-41 catalyst, *J. Environ. Chem. Eng.*, 2016, **4**, 47–55.
- 29 S. Karnjanakom, P. Maneechakr, C. Samart and G. Guan, A facile way for sugar transformation catalyzed by carbon-based Lewis-Brønsted solid acid, *Mol. Catal.*, 2019, **479**, 110632.
- 30 Q. Q. Zhou, L. Qiu and M. Q. Zhu, Eucommia ulmoides Oliver derived magnetic activated carbon for eliminating methylene blue from dyeing wastewater and its economic efficiency assessment, *Ind. Crops Prod.*, 2022, **187**, 115537.
- 31 Z. Zailan, M. Tahir, M. Jusoh and Z. Y. Zakaria, A review of sulfonic group bearing porous carbon catalyst for biodiesel production, *Renewable Energy*, 2021, **175**, 430–452.
- 32 X. Zhang, Y. Li, Y. He, D. Kong, B. Klein, S. Yin and H. Zhao, Co-pyrolysis characteristics of lignite and biomass and efficient adsorption of magnetic activated carbon prepared by co-pyrolysis char activation and modification for coking wastewater, *Fuel*, 2022, **324**, 124816.
- 33 Z. Wu, Q. Zheng, Y. Zhang, Y. Pang, T. Huang and D. Peng, Phosphorus recovery from waste-activated sludge through vivianite crystallization enhanced by magnetic biochar, *J. Cleaner Prod.*, 2023, **392**, 136294.
- 34 P. Maneechakr and S. Karnjanakom, Selective conversion of fructose into 5-ethoxymethylfurfural over green catalyst, *Res. Chem. Intermed.*, 2019, **45**, 743–756.
- 35 Q. Shi, S. Guo, J. Tang, H. Lyu, C. Ri and H. Sun, Enhanced removal of aged and differently functionalized polystyrene nanoplastics using ball-milled magnetic pinewood biochars, *Environ. Pollut.*, 2023, **316**, 120696.
- 36 P. Maneechakr and S. Karnjanakom, Facile utilization of magnetic MnO<sub>2</sub>@Fe<sub>3</sub>O<sub>4</sub>@sulfonated carbon sphere for selective removal of hazardous Pb(II) ion with an excellent capacity: Adsorption behavior/isotherm/kinetic/thermodynamic studies, *J. Environ. Chem. Eng.*, 2021, **9**, 106191.
- 37 N. A. Elessawy, M. H. Gouda, S. M. Ali, M. Salerno and M. S. M. Eldin, Effective Elimination of Contaminant Antibiotics Using High-Surface-Area Magnetic-Functionalized Graphene Nanocomposites Developed from Plastic Waste, *Materials*, 2020, **13**, 1517.
- 38 X. Cai, J. Li, Y. Liu, X. Hu, X. Tan, S. Liu, H. Wang, Y. Gu and L. Luo, Design and Preparation of Chitosan-Crosslinked Bismuth Ferrite/Biochar Coupled Magnetic Material for Methylene Blue Removal, *Int. J. Environ. Res. Public Health*, 2020, **17**, 6.
- 39 U. I. Nda-Umar, I. Ramli, E. N. Muhamad, N. Azri and Y. H. Taufiq-Yap, Optimization and Characterization of



- Mesoporous Sulfonated Carbon Catalyst and Its Application in Modeling and Optimization of Acetin Production, *Molecules*, 2020, **25**, 5221.
- 40 C. D. Dong, C. W. Chen, C. M. Kao, C. C. Chien and C. M. Hung, Wood-Biochar-Supported Magnetite Nanoparticles for Remediation of PAH-Contaminated Estuary Sediment, *Catalysts*, 2018, **8**, 73.
- 41 P. P. Upare, J. W. Yoon, M. Y. Kim, H. Y. Kang, D. W. Hwang, Y. K. Hwang, H. H. Kung and J. S. Chang, *Green Chem.*, 2013, **15**, 2935–2943.
- 42 G. P. Perez and M. J. Dumont, Production of HMF in high yield using a low cost and recyclable carbonaceous catalyst, *Chem. Eng. J.*, 2020, **382**, 12276.
- 43 F. Liu, M. Audemar, K. D. O. Vigier, D. Cartigny, J. M. Clacens, M. F. C. Gomes, A. A. H. Pádua, F. D. Campo and F. Jérôme, Selectivity enhancement in the aqueous acid-catalyzed conversion of glucose to 5-hydroxymethylfurfural induced by choline chloride, *Green Chem.*, 2013, **15**, 3205–3213.
- 44 C. Tempelman, U. Jacobs, J. Herselman, R. V. Driel, F. Schraa, J. Versijde, T. V. Waversveld, Y. Yagci, M. Barg, F. Smits, F. Kuijpers, K. Lamers, T. Remijn and V. Degirmenci, Waste apple biomass conversion to 5-HMF over tin doped sulfonated activated carbon as a catalyst, *Biomass Bioenergy*, 2023, **168**, 106661.
- 45 S. Mulk, M. Sajid, L. Wang, F. Liu and G. Pan, Catalytic conversion of sucrose to 5-hydroxymethylfurfural in green aqueous and organic medium, *J. Environ. Chem. Eng.*, 2022, **10**, 106613.
- 46 A. H. Jadhav, H. Kim and I. T. Hwang, Efficient selective dehydration of fructose and sucrose into 5-hydroxymethylfurfural (HMF) using dicationic room temperature ionic liquids as a catalyst, *Catal. Commun.*, 2012, **21**, 96–103.
- 47 Z. Babaei, A. N. Chermahini, M. Dinari, M. Saraji and A. Shahvar, Sulfonated triazine-based covalent organic polymer supported on mesoporous material: a new and robust material for the production of 5-hydroxymethylfurfural, *Sustainable Energy Fuels*, 2019, **3**, 1024–1032.
- 48 S. K. Das, S. Chatterjee, S. Mondal and A. Bhaumik, A new triazine-thiophene based porous organic polymer as efficient catalyst for the synthesis of chromenes *via* multicomponent coupling and catalyst support for facile synthesis of HMF from carbohydrates, *Mol. Catal.*, 2019, **475**, 110483.
- 49 R. Tomer and P. Biswas, Dehydration of glucose over sulfate impregnated ZnO (hexagonal-monoclinic) catalyst in dimethyl sulfoxide (DMSO) medium: Production, separation, and purification of 5-hydroxymethylfurfural (5-HMF) with high purity, *Catal. Today*, 2022, **404**, 219–228.
- 50 M. Li, W. Li, Y. Lu, H. Jameel, H. M. Chang and L. Ma, High conversion of glucose to 5-hydroxymethylfurfural using hydrochloric acid as a catalyst and sodium chloride as a promoter in a water/g-valerolactone system, *RSC Adv.*, 2017, **7**, 14330–14336.